Optical design of Cranz-Schardin cameras

Frank K. Lu
Xijing Liu
University of Texas at Arlington
Aerodynamics Research Center
Mechanical and Aerospace Engineering Department
Arlington, Texas 76019-0018
E-mail: lu@mae.uta.edu

Abstract. Cranz-Schardin cameras are low-cost, high-speed cameras. Although developed over 70 yr ago and available commercially, the design principles are not found in standard texts. Geometric optics are used to develop the design of a Cranz-Schardin camera. The design reveals the tight coupling between the light sources and the rest of the optics. The design of a light power gathering system is also described. The implementation of the design principles is illustrated by an actual camera capable of capturing four frames at a maximum rate of 1,000,000/s. [S0091-3286(97)02507-5]

Subject terms: cavitation; Cranz-Schardin camera; high-speed photography; light-emitting diodes; optics; shadowgraphy.

Paper 25106 received Oct. 21, 1996; revised manuscript received Feb. 24, 1997; accepted for publication Feb. 24, 1997.

1 Introduction

A conventional, high-speed camera such as a framing camera employs high-speed, rotating optomechanical components to sweep images on a stationary strip of film that is fastened to a cylindrical surface.[1,2] With all of its advantages, this kind of camera has a number of shortcomings. First, the high-speed, rotating, optomechanical components complicate design and manufacture, resulting in a costly device. Second, dark room work is needed to develop the negative film. Although recent developments in solid-state optoelectronics have produced advanced, high-speed imaging systems, these remain extremely expensive. A low-cost, high-speed camera, based on the Cranz-Schardin principle,[3] which uses instant film, can address the preceding shortcomings and is relatively inexpensive, may be adequate for some applications.

Basically, the Cranz-Schardin technique utilizes an array of point light sources, which is fired in sequence to provide both the light and the shutter action required to stop image movement during a dynamic event. This technique can be used for reflected or transmitted light photography. The principle of the method is illustrated in Figure 1 for transmitted light photography. In the figure, light from four point sources is expanded by a field lens L_1 and transmitted through the object. The light is then captured by lens L_2 and imaged by a camera at four distinct locations on the film plane.

Very high framing rates, in the order of millions per second, can be achieved. The framing rate can be varied according to a predetermined schedule tailored to the dynamic event. Thus, in the example shown in Figure 1, the individual light sources are triggered sequentially with an appropriate time delay between them. Nonequal time intervals are also feasible. In the Cranz-Schardin system, image splitting is achieved through the arrangement of light sources and the optical system. Frame rate and exposure time depend on the response time of the light sources and the drive circuit. But the exposure time is independent of framing rate. The image plane is a flat to which a photographic film can be placed.

The Cranz-Schardin camera is a low-cost alternative to other forms of expensive high-speed cameras. Although commercially available, the Cranz-Schardin camera is well suited for construction in a research laboratory. Since the Cranz-Schardin camera can record only a limited number of frames, much care must be exercised to synchronize the camera with other control and triggering components. With the ubiquitous presence of personal computers, it is now relatively easy to implement microprocessor control.[4]

While conventional, high-speed camera design theory and design methodology are well understood, unfortunately, the imaging mechanism of the Cranz-Schardin optical system is poorly addressed in the literature. An analysis of the Cranz-Schardin optical system based on geometric optics is developed. This analysis provides a design guide, revealing the relationships between the key optical components. The actual development of an innovative Cranz-Schardin high-speed camera with an efficient light gathering system and control of the diameter of the light beam are described. This camera, capable of a speed of 1,000,000 frames/s, is used in a cavitation experiment.

2 Optical Design

Image separation in the Cranz-Schardin camera is accomplished with a geometric arrangement of lenses and light sources. The most significant feature in the design of Cranz-Schardin cameras is, in fact, the light sources. The light sources are critical because they serve illumination and shutter functions. The camera requires an array of point light sources with a combination of lenses to separate the images. The point light sources should have good response, be easy to control, and they should be small. Since the development of the original Cranz-Schardin camera, various kinds of light sources have been used, namely, spark gaps[3] (as used in the original system), ruby lasers,[5] semiconductor lasers, and light-emitting diodes[6–8] (LEDs).

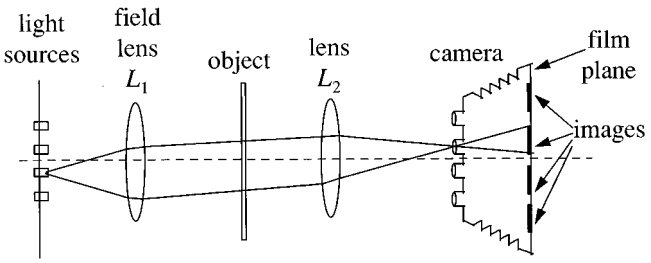

Fig. 1 Schematic illustrating the Cranz-Schardin principle.

The Cranz-Schardin principle, as illustrated in Figure 1, is easy to understand intuitively, but the actual imaging mechanism is rather complicated since there are a number of constraints that must be considered. It is usually desirable to obtain many images at the film plane. With commercially available sheet film sizes, numerous images means a reduced magnification ratio, and close arrangement and high quality of lenses. In fact, each of the lenses photographs the object from a different aspect. To reduce parallax, a highly compact arrangement of lenses and light sources is required. However, the physical dimensions of both light sources and lenses cannot be made too small so as to avoid overlapping of the images. Further, using LEDs as light sources, as in the present implementation, requires an efficient light-gathering system because of their weak emission. This slightly complicates the camera design. To develop a high performance camera, the designer needs to know the conjugate relationship of light sources, objective lenses, object, the film plane, as well as the factors that affect the magnification ratio, the size of viewing field, and the separation of images.

2.1 *Conjugate Relationship*

As is evident in Figure 1, the basic assumption in a conventional optical system there is a co-axis of lenses when the lenses are combined together does not hold in the Cranz-Schardin system. Thus the formation of images in a Cranz-Schardin system can be hard to understand. The key to understanding the imaging mechanism is to decompose the illumination and imaging systems.

For simplicity, the conjugate relation of the Cranz-Schardin camera is illustrated in Figure 2 by a two-source system. Light from point sources s_1 and s_2, located at the focal plane of the field lens L_1, is projected by this lens and another lens L_2 onto objectives l_1, and l_2, respectively;

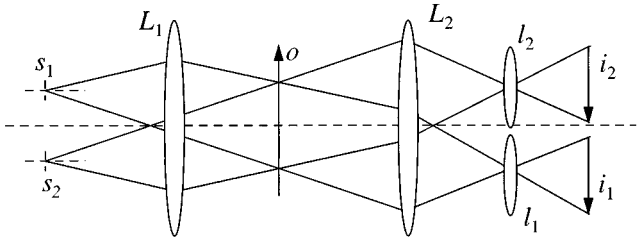

Fig. 2 Conjugate relationship for a two-source Cranz-Schardin system.

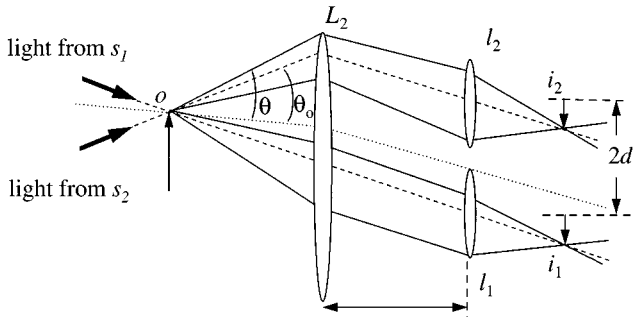

Fig. 3 Image separation.

s_1 is the conjugate of objective lens l_1, that is, s_1 is imaged on l_1. Similarly, s_2 is the conjugate of objective lens l_2. The object o, which is to be photographed is placed between L_1 and L_2, and is illuminated by the projected light beams. Object o is focused onto the film by field lens L_2 and objective lenses l_1 and l_2, respectively. Without object o (or, equivalently, if object o is nonrefracting), the image of s_1 at l_1 is a small light spot. On the film plane, the images of s_1 and s_2 are bright areas due to spreading of light beams. The size of the bright areas in the film plane determines the size of the viewing field.

Due to the presence of the object o, the actual image is a refraction light spot. This arrangement, where the light sources are the conjugate of objective lenses, ensures the smallest diameters of the objective lenses. Placing the light sources at the focal plane of field lens L_1 yields collimated beams. Object o, to be photographed, is placed at the common focal planes of L_1 and L_2. Since the viewing field is decided by the common area of all the projected light beams, the arrangement thus described achieves the largest viewing field.

Figure 3 illustrates the formation of the separated images. Collimated light from s_1 illuminates o, which refracts the light beam to form image i_1 at the film plane. Similarly collimated light from s_2 also illuminates o and the refracted light forms image i_2. In Figure 3, the dashed lines represent light paths without the object, and the solid lines represent light refracted by o. Usually, refraction is not very large, and light from s_1 refracted through o will almost focus onto i_1 and similarly for s_2 and l_2. If refraction is large, part of the light from s_1 incident on l_1 and part of the light from s_2 incident on i_2 will overlap. As can be deduced from Figure 3, if the angle of refraction is larger than θ, light from s_1 will be incident onto lens l_2, thereby interfering with the image from light source s_2. If the separation of objective lenses is $2d$ and the angle from the optical axis to the refracted light is θ, then it can be shown that

$$\tan(\theta-\theta_o)=\frac{d-f_2\tan\theta_o}{f_2}, \tag{1}$$

where θ_o is the angle of incidence light. For a given system, θ_o, d, and f_2 are constant. Hence, the image separa-

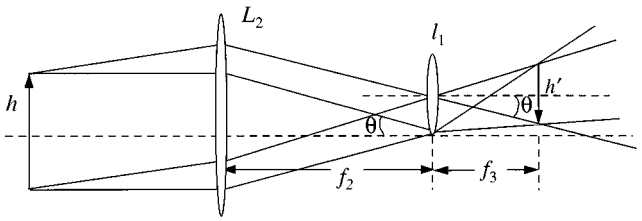

Fig. 4 Diagram showing the factors that affect the magnification ratio.

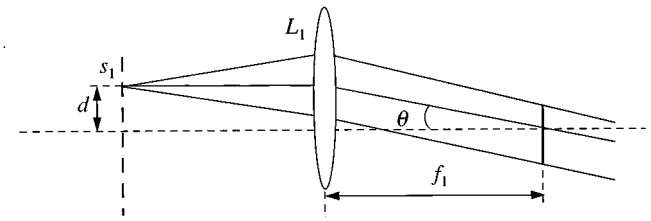

Fig. 5 Minimizing the angle of incidence of light.

tion condition is that the angle of refraction of object o is less than θ, which, from Equation (1), is given by

$$\theta = \theta_o + \arctan\left(\frac{d}{f_2} - \tan\ \theta_o\right). \tag{2}$$

This analysis shows that the Cranz-Schardin system is actually more effective in transmitted light photography than reflected light photography because, in such applications, the refraction of transmitted light is not very large. On the other hand, refraction of reflected light is usually large, and the Cranz-Schardin system is not so effective. Moreover, very bright light sources are needed for a reflected light system. It can be noted that in the literature L_2 is also called a field lens. This is not an accurate terminology. A field lens, by its definition, changes only the direction of light, and does not change the size of image. The preceding analysis indicates that L_2 definitely changes the size of the image.

2.2 *Magnification Ratio*

Suppose the object to be photographed is placed on the focal plane of L_2. Under this arrangement, the conjugate relationship is as shown in Figure 4; h is the height of the object, h' is the height of the image, f_2 is the focal length of lens L_2 and f_3 is the focal length of objective lens l_1. Hence,

$$\tan\ \theta = \frac{h}{2f_2} \quad \text{and} \quad \tan\ \theta = \frac{h'}{2f_3}, \tag{3}$$

and the magnification ratio is

$$\beta = \frac{h'}{h} = \frac{f_3}{f_2}. \tag{4}$$

Equation (4) shows that a large magnification ratio is achieved by increasing the focal length of the ojective lens l_1 or by decreasing the focal length of lens L_2. These focal lengths are subjected to a number of constraints, however. Due to the construction of thin lenses, the longer the focal length, the larger the diameter of the lens. Thus, an objective lens with a long focal length will have a large diameter. The limit to the diameter is determined by the size of available film, given that there is also a requirement for a certain number of images to be recorded. Decreasing the focal length of lens L_2 can also increase the magnification ratio. To obtain more images and a larger viewing field, the diameter of lens L_2 should be made larger. For the same reason, the focal length of L_2 cannot be decreased greatly. Usually, f_3 is smaller than f_2, so the magnification ratio β is less than unity. Large magnification ratio for high-speed photography is important since high-speed films do not produce fine quality prints when enlarged. For instant film, a large magnification ratio is more important because the photographs cannot be enlarged by ordinary means.

2.3 *Size of the Viewing Field*

Suppose the size of the film is W. Let the number of images in one dimension be n_r, the image size be w', the separation of objective lenses be $2d$, and the size of viewing field be w. If $W \geqslant 2n_r d$, to ensure that the images do not overlap,

$$w' = 2d, \quad w = w'/\beta \quad \text{and} \quad w = 2d/\beta. \tag{5}$$

Equation (5) shows that to obtain a large viewing field, the number of images and the magnification should be small. In other words, the magnification ratio is limited by the number of images, the size of the viewing field, and the characteristics of the lenses. Under these constraints, a large magnification ratio can be achieved by having an objective lens with a long focal length or having lens L_2 with a short focal length.

2.4 *Minimizing the Angle of Incidence of Light*

An inherent disadvantage of the Cranz-Schardin camera is that, with each image formed by light from one and only one light source, each image will photograph the object from a different aspect. To reduce this effect, the angle of incidence of the light on both the object and the camera lenses from the optical axis of the system should be minimized. One approach for minimizing the angle of incidence of light is to reduce the distance of the light sources and camera lenses. Limited by the physical dimensions of both light sources and camera lenses, the distance cannot be reduced greatly. Another approach is to increase the focal length of the field lens L_1.

As shown in Figure 5, the angle of incidence of light is θ, the focal length of L_1 is f_1 and light source separation is $2d$. Thus

$$\tan\ \theta = \frac{d}{f_1} \tag{6}$$

provides a criterion for f_1. A maximum angle of incidence 4 deg should be acceptable. Suppose $h = 76.2$ mm, then

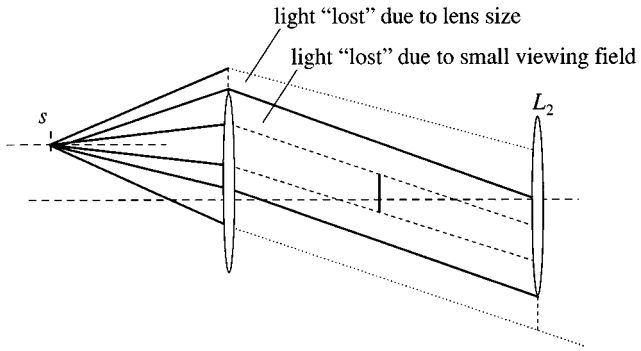

Fig. 6 Loss of light.

$$f_1 = 76.2/\tan 4 \ \deg = 1089.7 \ \text{mm}. \tag{7}$$

Some systems use a field lens with a focal length of 2000 mm to reduce the angle of incidence of light. Lenses with large focal length are expensive because they are difficult to manufacture. If d can be reduced, Equation (7) shows that the focal length of field lens L_1 can be shortened.

Lens L_2 should have the same parameters as field lens L_1. At least, the diameter D_2 of lens L_2 should be the same as L_1. The relative departure of a lens is defined as D/f. The manufacture of lenses with large D/f is difficult. For a given D/f, the focal length f_2 of L_2 should be made small to maximize the magnification ratio. This could be formalized as:

$$D_1 = D_2, \quad \frac{D_1}{f_1} \leqslant \frac{D_2}{f_2}. \tag{8}$$

In summary, the following relationships govern the design of a Cranz-Schardin camera:

$$\beta = \frac{f_3}{f_2}, \quad \tan\theta = \frac{d}{f_1}, \quad D_1 = D_2, \quad \frac{D_1}{f_1} \leqslant \frac{D_2}{f_2},$$
$$w = \frac{2d}{\beta}, \quad n_r = \frac{W}{2d}. \tag{9}$$

After deciding on the size of the viewing field, the preceding equations enable the maximum number of images, the largest magnification ratio and the smallest angle of incidence to be obtained for the Cranz-Schardin camera.

2.5 *A Light-Gathering Power System*

The efficiency of light transmission through the optical system can also be improved. Due to the limited diameter of the lenses, not all light from a source is collected. Further, a small viewing field will reduce light collection. In Figure 6, the light between the outside dotted lines and the solid lines is lost due to the limitation of lens sizes, while the light between the inside dotted lines and the solid lines is lost due to the small viewing field. Thus, it is important to use bright light sources. Nevertheless, it is important that the optical system is designed carefully so as to collect as much light as possible. To improve light collection, a collection lens with a short focal length is inserted between each light source and field lens L_1. After insertion of collection lenses, the light transmitted through the optical system is shown in Figure 7. The collection lens l is placed at the focal plane of the field lens L_1. The virtual image of light source s formed by collection lens l is s'. From the object, light rays emerge as if they still came from a point source placed on the focal plane of field lens L_1, but the structure of light rays is changed, and the light cone is greatly compacted. If the apertures of the collection lenses are large enough, light from the sources can be collected completely by the collection lenses and transmitted through the optical system. This system greatly improves the efficiency of the light transmitted through the optical system. By adjusting the distances between the collection lenses and the field lens, the diameter of the light beam can be controlled and, therefore, the viewing field can be controlled without changing the optical system.

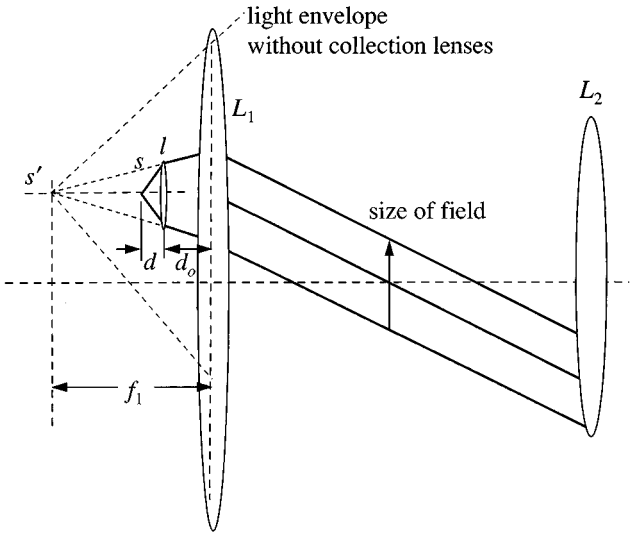

Fig. 7 Light transmission after insertion of collection system.

The aperture of a collection lens characterizes its ability to collect light. To collect as much light as possible, the collection lens must have as large an aperture as possible. The aperture is defined as D/f. For a practical arrangement, D cannot be large. Thus, the only way to increase the aperture is to shorten the focal length of the collect lens. In fact, the focal length of collection lenses should be reasonably short to leave enough space for inserting light sources before them. If a small viewing field is required, the diameter of collection lenses should be small, and the distance between collection lenses l and the field lens L_1 should be short. If a large viewing field is required, the diameter of collection lenses and the distance between collection lenses l and the field lens L_1 should be large.

If the diameter and the focal length of the collection lens are D and f_c, given the size of viewing field W, the distances d and d_o can be decided by the following formulas:

$$\frac{1}{d} - \frac{1}{f_1 - d_o} = \frac{1}{f_c}, \quad \frac{W}{D} = \frac{1}{f_1 - d_o}. \tag{10}$$

From Equations (10)

$$d_o=\left(1-\frac{D}{W}\right)f_1, \quad d=\frac{f_c f_1 D}{f_c W+f_1 D}. \tag{11}$$

3 Implementation

A Cranz-Schardin camera, designed according to the principles just outlined, was constructed to study transient, shock–bubble interactions.[9] Following the work of Refs. 6 and 8, this camera used high-powered LEDs as light sources. Specifically, these LEDs were Hewlett Packard Model HLMA-CH00, which used newly developed aluminum indium gallium phosphide (AlInGaP) technology. The main advantages of this type of LED are that it has a very high luminous intensity, typically 3000 mcd at a current of 20 mA, and a narrow viewing angle of 7 degs. The LED emits red light at a peak wavelength of 615 nm. The LED is available with a 5 mm diameter lens. In applications where the field of view is smaller than these ''point sources,'' special consideration must be given to reduce the size of the beam cross section to the field of view. The LEDs and the camera apertures were arranged in two staggered rows to ensure that the images do not interfere, while still preserving the design requirements for minimum parallax.

The LEDs were driven by a special, four-channel pulsed power generator (Model AV-106C-PS-P-UTA2, Avtech Electrosystems, Ottawa, Canada). Each channel of the pulsed power generator can deliver a maximum current of 10 A at a maximum load voltage of 100 V to drive the LEDs. Pulse width is variable from 0.5 to 20 μs, with a rise or fall time of less than 50 ns. The pulses could be delayed from 1 to 20 μs between channels. A dc mode, which provided continuous power, was used to adjust the optical setup. This power generator yielded good exposures on high-speed instant film (Polaroid Type 57, ISO 3000) under 1 A current and 1 μs pulse width. An example of LED outputs is shown in Figure 8. LED outputs were detected using a United Detector Technology (Hawthorne, California) Model HS040 ultrafast photodetector, which has a typical response time of 0.8 ns. The photodetector was placed on the common area of light beams from four different LEDs behind a diffuser at the film plane. The width of optical pulse provided the exposure time. The frame rate is independent of exposure time. The time delay between different channels was set to the minimum and, therefore, a subsequent pulse was initiated before the previous one ended. This is indicated as an overlap in the photodetector output in Figure 8. With a time interval of 1 μs between pulses, the maximum frame rate of 1,000,000 frames/s was achieved in this case. A light-gathering power system was also used. Considering the commercial availability of

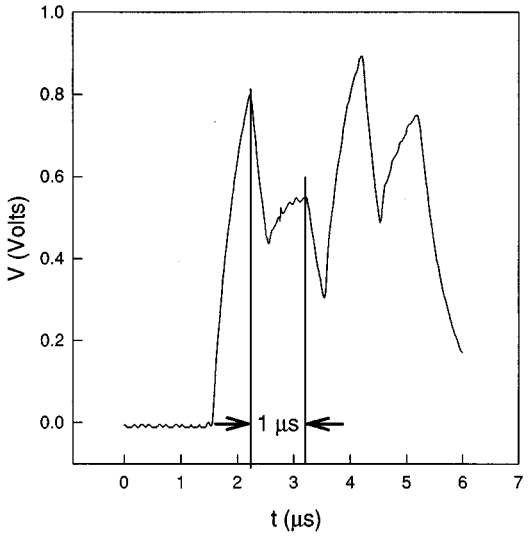

Fig. 8 LED outputs: pulse current=3 A, current pulse width=1 μs, zero time delay between channels; 1,000,000 frames/s, optical pulse width=1.5 μs.

lenses and their costs, the lenses that were chosen are listed in Table 1. Under this design, the magnification ratio is

$$\beta=f_3/f_2=195/250=0.78.$$

The experiments for studying bubble collapse due to shock impact were carried out in a miniature shock tube of rectangular cross section. A schematic of the experimental apparatus is shown in Figure 9. The 130 mm long shock tube, which had a 1.5 mm wide $\times$8 mm high cross section, was separated from the high pressure chamber by an electromagnetic plunger. The shock tube was filled with tap water and a bubble of 5 to 6 mm was implanted toward the open end. When the plunger was retracted, high pressure air was released into the shock tube. A shock propagated ahead of the air into the water. This shock was detected by a sensor. The signal was then used to trigger the pulse generator, which fired the LEDs in sequence. The time delay between shock detection and triggering of the LEDs could be adjusted and preliminary calibrations were performed to determine the appropriate delay. An example of a sequence of shadowgraph images is shown in Figure 10. The camera was operated at 50,000 frames/s with equal optical pulse widths of 4 μs. The bubble diameter was 6 mm and the shock pressure was 0.12 MPa. The weak shock could not be detected in the shadowgraphs. Nevertheless, it is clear that the shock, impinging from the left, produced a microjet that penetrated the bubble. Two counter-rotating mi-

Table 1 Lens characteristics.

	Field Lens L_1	Lens L_2	Four Objective Lenses	Four Collection Lenses
Focal length (mm)	250	250	195	15
Diameter (mm)	150	150	15	12
Type	plano-convex	plano-convex	plano-convex	aspheric condenser

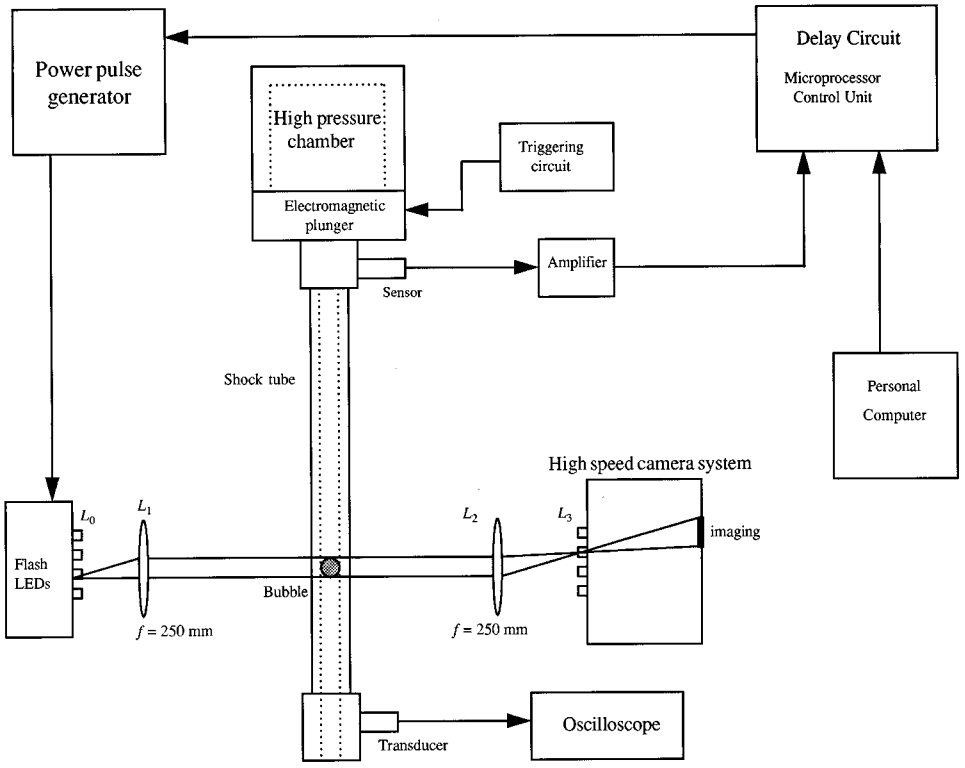

Fig. 9 Schematic of confined shockbubble experiment.

crobubbles were formed as the jet exited the bubble [Fig. 10(d)]. Moreover, two counter-rotating vortices were shed into the water, these being visible as dark lobes on the right of the microbubble pair. The four frames, unfortunately, were inadequate to build up the entire collapse sequence. From composite photographs, the bubbles were found to collapse in 100 to 140 μs.

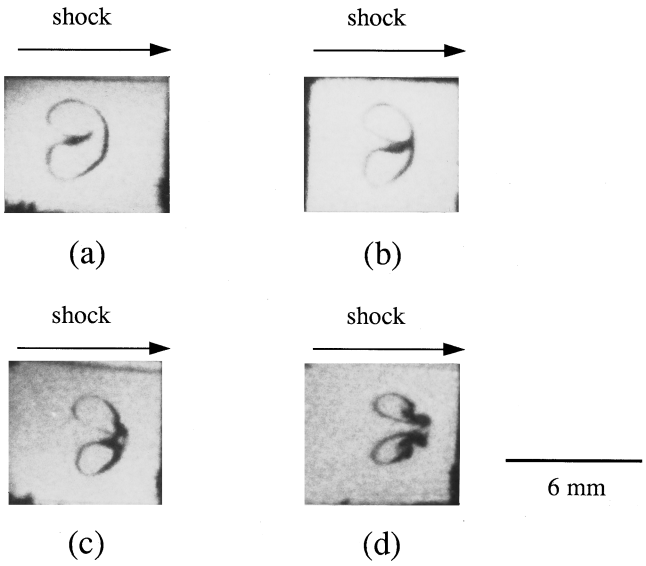

Fig. 10 Example of shadowgraph images using a Cranz-Schardin camera.

4 Conclusions

The design principles for a Cranz-Schardin camera have been clearly defined for the first time in the literature, even though such cameras have been in use for about 70 yr. The complexity of the camera due to the tight coupling between the illumination and imaging components is analyzed. A light-gathering system is incorporated in the design. The various constraints to the camera, such as magnification ratio, size of lenses, etc., have been elucidated. Based on the design, an actual Cranz-Schardin camera, using high-powered LEDs as light sources, and capable of acquiring four images at a maximum framing rate of 1,000,000/s, was developed and briefly described. The camera was used for the study of shock-induced collapse of cavitation bubbles.

Acknowledgments

The authors gratefully acknowledge support of this work by the Texas Higher Education Coordinating Board's Advanced Research Program, Project no. 003656-004. We would like to express our thanks to Jim Holland, Binu Kurian and Xiuyan Zhang for helping with the experiments. We also like to thank Hewlett-Packard for providing the initial sample of LEDs.

References

1. W. G. Hyzer, *Engineering and Scientific High-Speed Photography*, Macmillan, New York (1962).
2. A. S. Dubovik, *Photographic Recording of High-Speed Processes*, rev. ed., Wiley, New York (1981).
3. C. Cranz and H. Schardin, ''Kinematographie auf ruhendem Film und mit extrem hoher Bildfrequenz,'' *Z. Phys.* **56**, 147–183 (1929).
4. B. Stasicki and G. E. A. Meier, ''A computer controlled ultra high-

speed video camera system,'' in *Proc. SPIE* **2513**, 196–208 (1995).
5. J. W. Dally and R. J. Sanford, ''Multiple ruby laser system for high speed photography,'' *Opt. Eng.* **21**, 704–708 (1982).
6. B. Stasicki, W. J. Hiller, and G. E. A. Meier, ''Light pulse generator for high speed photography using semiconductor devices as a light source,'' *Opt. Eng.* **29**, 821–827 (1990).
7. B. Bretthauer, G. E. A. Meier, and B. Stasicki, ''An electronic Cranz-Schardin camera,'' *Rev. Sci. Instrum.* **62**, 364–368 (1991).
8. W. Hiller, H. M. Lent, G. E. A. Meier, and B. Stasicki, ''A pulsed light generator for high speed photography,'' *Exper. Fluids* **5**, 141–144 (1987).
9. F. K. Lu, X. Zhang, and X. Liu, ''Visualization of confined shock–bubble interactions,'' submitted for publication.

Frank K. Lu obtained his PhD in mechanical engineering from the Pennsylvania State University in 1988. He joined the University of Texas at Arlington in 1987 and is presently an associate professor in the Mechanical and Aerospace Engineering Department and the director of its Aerodynamics Research Center. His primary research interests are in fluid mechanics and gasdynamics. His recent research involves hypervelocity facility and instrument development, detonations, cavitation, and laser-induced fluorescence.

Xijing Liu received the BS and MS degrees in applied optics and optical engineering from the Harbin Institute of Technology, China, in 1984 and 1987, respectively. He received his master's degree in computer science and engineering from the University of Texas at Arlington (UTA) in 1996. From 1987 until 1993, he worked for Anshan Iron and Steel Complex, China, where he conducted research in optical fiber probes and production automation control. From 1994 to 1996 he worked at the Aerodynamics Research Center of UTA to develop visualization methods for studying shock wave interactions with bubbles. Currently, he is working with Omnipoint Corporation, Fort Worth, Texas, in software engineering. His research interests include optical instrumentation and computer software engineering. He is a member of IEEE.